

Three-Dimensional Spin Fluctuations in $\text{Na}_{0.75}\text{CoO}_2$

L. M. Helme,^{1,*} A. T. Boothroyd,¹ R. Coldea,¹ D. Prabhakaran,¹ D. A. Tennant,² A. Hiess,³ and J. Kulda³

¹*Department of Physics, University of Oxford, Oxford OX1 3PU, United Kingdom*

²*School of Physics and Astronomy, University of St. Andrews, St. Andrews, Fife KY16 9SS, United Kingdom*

³*Institut Laue-Langevin, BP 156, 38042 Grenoble CEDEX 9, France*

(Received 18 October 2004; published 22 April 2005)

We report polarized- and unpolarized-neutron scattering measurements of magnetic excitations in single-crystal $\text{Na}_{0.75}\text{CoO}_2$. The data confirm ferromagnetic correlations within the cobalt layers and reveal antiferromagnetic correlations perpendicular to the layers, consistent with an *A*-type antiferromagnetic ordering. The magnetic modes propagating perpendicular to the layers are sharp, and reach a maximum energy of ~ 12 meV. From a minimal spin-wave model, containing only nearest-neighbor Heisenberg exchange interactions, we estimate the interlayer and intralayer exchange constants to be 12.2 ± 0.5 meV and -6 ± 2 meV, respectively. We conclude that the magnetic fluctuations in $\text{Na}_{0.75}\text{CoO}_2$ are highly three dimensional.

DOI: 10.1103/PhysRevLett.94.157206

PACS numbers: 75.40.Gb, 74.20.Mn, 74.25.Ha, 78.70.Nx

Its potential as a battery electrode material [1] and in thermoelectric devices [2], and most recently the discovery of superconductivity after hydration [3], have made the layered cobaltite Na_xCoO_2 the subject of intense research in the last few years. The structure comprises two-dimensional layers of CoO_2 separated by layers of sodium ions, with the Co atoms forming a triangular lattice [4]. The superconducting compound $\text{Na}_x\text{CoO}_2 \cdot y\text{H}_2\text{O}$ ($x \approx 0.3$, $y \approx 1.3$, $T_c \approx 4.5$ K) is of particular interest as the first cobalt-oxide based superconductor [3]. The layered structure and the existence of superconductivity over a narrow range of doping [5] near to a Mott insulator invite comparisons with the copper-oxide superconductors, and evidence is mounting for an unconventional mechanism of superconductivity [6].

In common with the superconducting cuprates, the properties of the normal metallic state of Na_xCoO_2 are unusual and show effects due to strong electronic correlations. One of the outstanding puzzles is the nature of the magnetic interactions, which may play a central role in the formation of the superconducting state. In the range $x \sim 0.7$ – 0.95 the susceptibility of Na_xCoO_2 shows a sharp magnetic transition at $T_m \approx 22$ K [7,8]. Muon-spin rotation measurements confirmed the existence of static magnetic order below T_m , and placed an upper limit of $0.2\mu_B$ on the size of the ordered moment [9]. For $T > T_m$ the susceptibility can be fitted to a Curie-Weiss law plus a constant term, which indicates a degree of local character to the magnetism [7]. Such fits give negative Weiss temperatures, implying dominant antiferromagnetic correlations. However, a recent neutron scattering study of $\text{Na}_{0.75}\text{CoO}_2$ found strong ferromagnetic spin correlations within the cobalt-oxide layers [10], consistent with several theoretical predictions [11]. Until now there have been no measurements of magnetic fluctuations perpendicular to the layers, and the nature of the magnetic order below T_m has not been established.

Here we investigate further the magnetic correlations in $\text{Na}_{0.75}\text{CoO}_2$, using both polarized- and unpolarized-neutron scattering. The new data reveal strong antiferromagnetic correlations perpendicular to the cobalt-oxide layers, consistent with an *A*-type antiferromagnetic ordering. Surprisingly, the interlayer exchange coupling is found to be similar in strength to the intralayer coupling, so that despite the layered structure the magnetic interactions are highly three dimensional.

The measurements were made on a single crystal of $\text{Na}_{0.75}\text{CoO}_2$ grown in Oxford by the floating-zone method [12]. For the neutron studies, we cleaved a crystal of mass ~ 1.5 g from a zone-melted rod. Smaller crystals from the same rod were examined by x-ray diffraction, magnetometry and electron microscopy. The analysis revealed the presence of small inclusions of cobalt oxides (CoO and Co_3O_4), consistent with previous reports for melt-grown crystals [13]. These impurity phases, which amounted to a few percent of the total, were found by neutron diffraction to grow epitaxially on the host lattice. Once the orientation of the impurity crystallites had been determined, it was straightforward to distinguish the impurity signal from that of the host. The anisotropic magnetic susceptibility of the crystals exhibited an anomaly at $T_m \approx 22$ K for fields applied parallel to the *c* axis, consistent with the magnetic transition observed previously [7].

Unpolarized- and polarized-neutron scattering measurements were performed on the thermal triple-axis spectrometers IN8 and IN20, respectively, at the Institut Laue-Langevin. On IN8 we employed a Si(111) monochromator and a pyrolytic graphite (002) analyzer, and worked with a fixed final energy $E_f = 14.7$ meV. To increase the count rate, both the monochromator and analyzer were curved horizontally and vertically for optimum focusing. For the polarized-neutron measurements on IN20, we used curved Heusler (111) as both monochromator and analyzer, and $E_f = 34.8$ meV. On both instruments a graphite filter was

placed in the scattered beam to suppress higher order harmonics. The crystal was mounted in a standard helium cryostat, and most of the measurements were made within the (100)–(001) scattering plane. Here, the notation (hkl) represents the wave vector $\mathbf{Q} = h\mathbf{a}^* + k\mathbf{b}^* + l\mathbf{c}^*$, where \mathbf{a}^* , \mathbf{b}^* , and \mathbf{c}^* are the basis vectors of the hexagonal reciprocal lattice (the angle between \mathbf{a}^* and \mathbf{b}^* is 60°) [14].

Our previous studies [10] showed that the magnetic excitation spectrum of $\text{Na}_{0.75}\text{CoO}_2$ is centered on the Γ point of the two-dimensional Brillouin zone, i.e., (00), corresponding to ferromagnetic correlations within the cobalt-oxide layers. In the present work, we concentrated on the out-of-plane wave vector component of the magnetic fluctuations.

Figure 1(a) shows an example scan parallel to the $(00l)$ direction performed on IN8 at a fixed energy transfer of 7 meV. Two peaks can be seen symmetrically on either side of $l = 3$. Figure 1(b) displays the same scan but this time performed on IN20 with the neutron polarization maintained parallel to the scattering vector during the scan. In this configuration the spin-flip (SF) scattering is purely magnetic, and the non-spin-flip (NSF) scattering is non-magnetic. The two peaks are clearly present in the SF channel and absent from the NSF channel. The peaks are essentially resolution limited, as indicated, but are less well

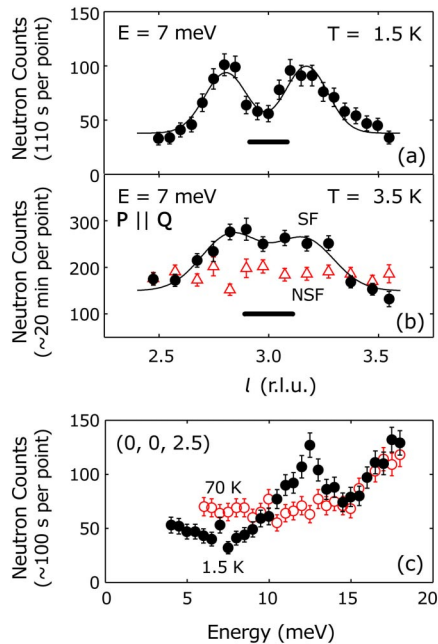


FIG. 1 (color online). Magnetic scattering from $\text{Na}_{0.75}\text{CoO}_2$. Panels (a) and (b) show scans parallel to $(00l)$ made at a fixed energy of 7 meV. Panel (c) displays energy scans made at the zone boundary $l = 2.5$ at temperatures of 1.5 and 70 K. The data in (a) and (c) were obtained with unpolarized neutrons on IN8 using a fixed final energy of $E_f = 14.7$ meV. The data in (b) are the SF and NSF scattering collected on IN20 with the neutron polarization \mathbf{P} parallel to the scattering vector \mathbf{Q} and with fixed $E_f = 34.8$ meV. The horizontal bars in (a) and (b) indicate the experimental resolution.

resolved in Fig. 1(b) than in Fig. 1(a) because of the larger neutron energy used on IN20. We conclude that the peaks arise from magnetic excitations.

The scan shown in Fig. 1(a) was repeated for different fixed energies between 3 and 10 meV. Each scan contained two peaks symmetric about (003), with the peak separation increasing with increasing energy. In addition, energy scans were made at several fixed points along the line $(00l)$. Figure 1(c) shows one such scan, made at $l = 2.5$, the zone boundary in the out-of-plane direction. The scan was performed at 1.5 K and then repeated at 70 K. The prominent peak at ~ 12 meV in the low temperature scan has disappeared by 70 K. This again confirms the magnetic origin of the scattering since magnetic correlations are destroyed with increasing temperature.

By fitting Gaussian functions to the peaks in both types of scan, we constructed the magnon dispersion relation. This is displayed in Fig. 2. There is clearly a mode dispersing from (003) with a maximum energy of approximately 12 meV. The crystal structure of Na_xCoO_2 is such that no structural Bragg peaks are allowed for positions $(00l)$ with odd l . As expected, therefore, no structural Bragg peak was observed at (003), but scans made at different temperatures revealed no magnetic Bragg peak at this point either.

The simplest spin arrangement consistent with the observations is the *A*-type antiferromagnet shown in Fig. 2, in which the spins are ordered ferromagnetically within the layers and the layers are coupled antiferromagnetically along the c axis. Each cobalt ion is taken to have the same spin. For no magnetic Bragg peak to appear at (003), the spins must be parallel or antiparallel to the c axis [15]. This is because neutrons do not couple to spin components parallel to the scattering vector.

To analyze the three-dimensional dispersion in more detail, we compare the experimental results with a spin-

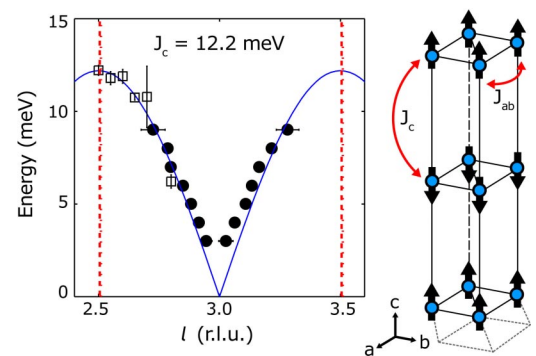


FIG. 2 (color online). Left: The magnon dispersion of $\text{Na}_{0.75}\text{CoO}_2$ parallel to $(00l)$ measured on IN8 at a temperature of 1.5 K. Solid circles are from constant-energy scans, e.g., Fig. 1(a), and open squares are from constant- l scans, e.g., Fig. 1(c). The solid curve is calculated from the spin-wave dispersion Eqs. (2) and (3) with exchange constant $J_c = 12.2$ meV. Dotted lines show the zone boundaries. Right: The magnetic structure on which the spin-wave model is based, showing the two exchange constants J_{ab} and J_c , and the spin direction.

wave model containing the minimum number of exchange parameters. The Hamiltonian is taken to be

$$\mathcal{H} = J_{ab} \sum_{\langle i, i' \rangle} \mathbf{S}_i \cdot \mathbf{S}_{i'} + J_c \sum_{\langle i, j \rangle} \mathbf{S}_i \cdot \mathbf{S}_j, \quad (1)$$

where J_{ab} and J_c are intralayer and interlayer exchange parameters, respectively, as indicated in Fig. 2. Only nearest-neighbor interactions are included in the summations, and $\langle i, i' \rangle$ and $\langle i, j \rangle$ denote spin pairs within the same layer and on adjacent layers, respectively.

Standard methods were used to derive the spin-wave dispersion and scattering cross section from the Hamiltonian. The resulting expression for the spin-wave energy dispersion is

$$\hbar\omega_{\mathbf{k}} = 2S\sqrt{(J_{\mathbf{k}} - J_{\mathbf{k}_m})[(J_{\mathbf{k}-\mathbf{k}_m} + J_{\mathbf{k}+\mathbf{k}_m})/2 - J_{\mathbf{k}_m}]}, \quad (2)$$

where S is the spin (here assumed to be $S = 1/2$), \mathbf{k} is the magnon wave vector, and $\mathbf{k}_m = (001)$ is the propagation vector of the magnetic structure. $J_{\mathbf{k}}$ is the Fourier transform of the exchange couplings, given by

$$J_{\mathbf{k}} = J_c \cos(\pi l) + J_{ab} \{\cos(2\pi h) + \cos(2\pi k) + \cos[2\pi(h+k)]\}, \quad (3)$$

with $J_{\mathbf{k}_m}$, $J_{\mathbf{k}-\mathbf{k}_m}$, and $J_{\mathbf{k}+\mathbf{k}_m}$ defined in a similar manner.

The dispersion relation along the $(00l)$ direction does not depend on J_{ab} , so by comparing the spin-wave dispersion to the data in Fig. 2 we can immediately obtain a value for J_c . The best fit is shown by the solid curve in Fig. 2, which is calculated with $J_c = 12.2$ meV. At low energies the data points lie systematically above the fitted curve, suggesting the presence of a small gap of 1–2 meV. Apart from this, the model provides a good description of the data.

The measurements described so far probe only the interplane correlations. To gain quantitative information on correlations within the planes, we apply the model to the results obtained previously [10] with a crystal of the same composition using the MAPS time-of-flight spectrometer at ISIS. Figure 3(a) reproduces part of a slice through the MAPS data from Ref. [10], in which the data were averaged over energy transfers $E = 8$ –12 meV. The configuration used on MAPS is such that the out-of-plane wave vector component l varies with E . For this slice $l \approx 1$.

To continue the analysis, a MAPS-style data set was simulated from the model to allow direct comparison with the MAPS data. The MAPS data set is an intensity array in (\mathbf{Q}, E) space, so for each data point in this space the simulated intensity was calculated, including the magnetic form factor and orientation factor [16]. For the calculation, J_c was fixed to the value 12.2 meV determined from the interlayer dispersion, while J_{ab} was varied until good agreement between simulation and experiment was achieved.

Following this procedure we determined that $J_{ab} = -6 \pm 2$ meV. Figure 3(b) shows a slice through the simulated data for $J_{ab} = -6$ meV and $J_c = 12.2$ meV to give

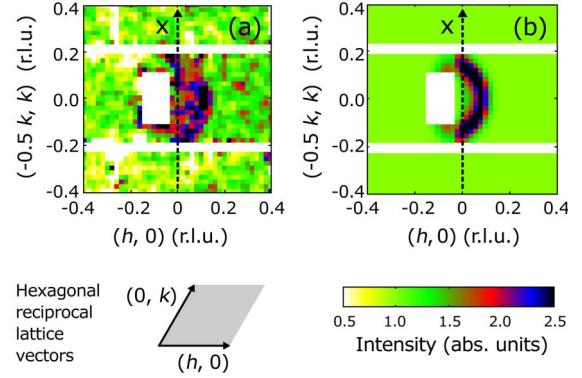


FIG. 3 (color online). (a) Neutron inelastic scattering from $\text{Na}_{0.75}\text{CoO}_2$ recorded on the MAPS spectrometer at ISIS with an incident energy of 60 meV [10]. The map contains data averaged over energy transfers of 8–12 meV and is projected onto the (h, k) reciprocal lattice plane of the crystal. (b) Simulated intensity using the model described in the text with $J_{ab} = -6$ meV and $J_c = 12.2$ meV. The axis labels correspond to the hexagonal reciprocal axes drawn in the figure.

direct comparison with Fig. 3(a). The distribution of scattering within the plane is well reproduced by the model. Figure 4 shows constant-energy cuts through both real and simulated data sets along the line marked X in Fig. 3, at three different energies. The model does not include the variation of the background with energy, so a flat background was fitted for each energy independently. In addition, the overall scattering amplitude had to be systematically reduced with increasing energy to fit the data satisfactorily. This reduction, which was nearly a factor of 2 over the energy range 6.5–14 meV, is not predicted by the spin-wave model.

The measurements and calculations reported here reveal that the magnetic correlations in $\text{Na}_{0.75}\text{CoO}_2$ are of a three-dimensional nature, despite its highly 2D physical properties. In fact, the interplane exchange constant J_c is found to be roughly double the intraplane constant J_{ab} . The spin-wave modes propagating along the c axis are found to be sharp, indicating a well correlated ground state. The in-plane modes exhibit some broadening, as indicated on Fig. 4 and reported previously [10].

Comparisons have been made between Na_xCoO_2 and other layered superconducting families, such as the copper oxides. The strong 2D nature of the cuprates is thought to be important for their superconductivity, and contrasts with the 3D magnetic interactions found here for Na_xCoO_2 . It is likely that the c -axis magnetic coupling is weakened in hydrated Na_xCoO_2 , due to the large interlayer spacing, and it is tempting to speculate that this coupling actually inhibits superconductivity. This possibility makes the present observations especially pertinent given recent evidence for the presence of H_3O^+ ions in the hydrated compound, which would make the doping level for superconductivity similar to that in $\text{Na}_{0.75}\text{CoO}_2$ [17].

The spin excitation spectrum observed here is not easily reconciled with the usual picture of localized Co^{4+} and

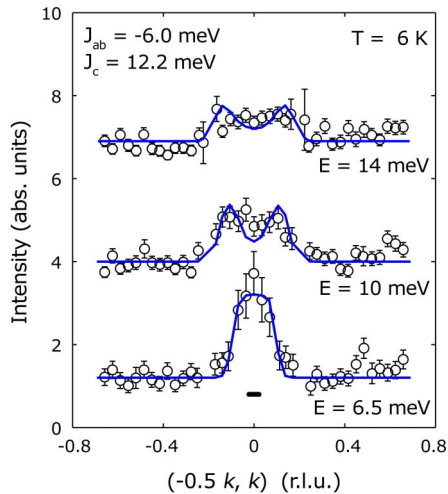


FIG. 4 (color online). Constant-energy cuts taken along the line marked X in Fig. 3. Open circles show neutron data points, while the solid lines are from the simulation. The 10 and 14 meV data have been displaced vertically by 3 and 6 units, respectively. The horizontal bar indicates the resolution.

Co^{3+} ions carrying spins $S = 1/2$ and $S = 0$, respectively. If localized Co^{4+} spins were distributed at random, then a very broad magnetic excitation spectrum would be expected, unlike the sharp modes observed experimentally. One possibility is that there is a phase separation into ferromagnetic in-plane clusters of Co^{4+} ions in a matrix of nonmagnetic Co^{3+} . However, the Coulomb penalty would be considerable, and to obtain consistency with the observed sharp spin modes along the c axis these clusters would have to be aligned vertically above each other over many layers.

An alternative suggestion based on optical conductivity data [18] is that $\text{Na}_{0.75}\text{CoO}_2$ might have a stable Wigner crystal ground state, with Co^{4+} spins on a triangular lattice of side $2a$ in a background of Co^{3+} . This would double the period of the magnetic correlations within the layers and hence create magnetic zone centers at the M points, e.g., $(\frac{1}{2}00)$, of the Brillouin zone. Since no magnetic excitations are observed emerging from the M points [10], we can rule out this type of charge order in $\text{Na}_{0.75}\text{CoO}_2$, at least in the simplest case where the Co^{3+} ions are nonmagnetic. The Wigner crystal model can only be reconciled with the observed spin excitation spectrum if the Co^{3+} ions carry a moment of similar size to the Co^{4+} ions and all moments interact ferromagnetically.

With these points in mind, it might be that a more metallic picture should be sought, in which the Co atoms have no or only a small disproportionation of charge. This would naturally produce a similar magnetic moment on each site, consistent with the model of an A -type antiferromagnet assumed here. In particular, a weakly itinerant

ground state with strong spin fluctuations could reconcile the small ordered moment and low ordering temperature with the relatively large energy scale of the spin excitation spectrum, and account for the broadening and intensity loss of the spin modes with increasing energy.

Finally, we note that similar results to ours have very recently been reported by Bayrakci *et al.* [19] on a crystal of $\text{Na}_{0.82}\text{CoO}_2$.

We acknowledge informative discussions with C. Bernhard, P. Bourges, B. Keimer, G. Khaliullin, N. Kovaleva, and R. McKenzie. We would like to thank the University of Oxford, the ISIS facility, and the Engineering and Physical Sciences Research Council of Great Britain for financial support.

*Electronic address: l.helme1@physics.ox.ac.uk

- [1] M. M. Doeff *et al.*, *Electrochim. Acta* **40**, 2205 (1995).
- [2] I. Terasaki *et al.*, *Phys. Rev. B* **56**, R12685 (1997).
- [3] K. Takada *et al.*, *Nature (London)* **422**, 53 (2003).
- [4] R. J. Balsaks and R. L. Davis, *Solid State Ionics* **93**, 279 (1997); Q. Huang *et al.*, *Phys. Rev. B* **70**, 184110 (2004).
- [5] R. E. Schaak *et al.*, *Nature (London)* **424**, 527 (2003).
- [6] M. Kato *et al.*, cond-mat/0306036; T. Fujimoto *et al.*, *Phys. Rev. Lett.* **92**, 047004 (2004); K. Ishida *et al.*, *J. Phys. Soc. Jpn.* **72**, 3041 (2003); W. Higemoto *et al.*, *Phys. Rev. B* **70**, 184110 (2004); Y. Kobayashi, M. Yokoi, and M. Sato, *J. Phys. Soc. Jpn.* **72**, 2161 (2003).
- [7] T. Motohashi *et al.*, *Phys. Rev. B* **67**, 064406 (2003).
- [8] D. Prabhakaran *et al.*, cond-mat/0312493; B. C. Sales *et al.*, cond-mat/0402379.
- [9] J. Sugiyama *et al.*, *Phys. Rev. B* **67**, 214420 (2003); S. P. Bayrakci *et al.*, *Phys. Rev. B* **69**, 100410(R) (2004).
- [10] A. T. Boothroyd *et al.*, *Phys. Rev. Lett.* **92**, 197201 (2004).
- [11] D. J. Singh, *Phys. Rev. B* **61**, 13397 (2000); **68**, 020503(R) (2003); G. Baskaran, *Phys. Rev. Lett.* **91**, 097003 (2003); B. Kumar and B. S. Shastry, *Phys. Rev. B* **68**, 104508 (2003); K.-W. Lee, J. Kuneš, and W. E. Pickett, *Phys. Rev. B* **70**, 045104 (2004); M. Mochizuki, Y. Yanase, and M. Ogata, cond-mat/0407094 [*Phys. Rev. Lett.* (to be published)].
- [12] D. Prabhakaran *et al.*, *J. Cryst. Growth* **271**, 74 (2004).
- [13] F. C. Chou *et al.*, cond-mat/0405158.
- [14] The lengths are $|\mathbf{a}^*| = |\mathbf{b}^*| = 4\pi/(a\sqrt{3})$ and $|\mathbf{c}^*| = 2\pi/c$, with $a = 2.83 \text{ \AA}$ and $c = 10.8 \text{ \AA}$ at room temperature.
- [15] Magnetic Bragg peaks could not be observed at other expected positions either, but these were contaminated with relatively strong nuclear elastic scattering which probably swamped the weak magnetic Bragg scattering.
- [16] G. L. Squires, *Introduction to the Theory of Thermal Neutron Scattering* (Cambridge University Press, Cambridge, England, 1978).
- [17] C. J. Milne *et al.*, *Phys. Rev. Lett.* **93**, 247007 (2004).
- [18] C. Bernhard *et al.*, *Phys. Rev. Lett.* **93**, 167003 (2004).
- [19] S. P. Bayrakci *et al.*, preceding Letter, *Phys. Rev. Lett.* **94**, 157205 (2005).